

Toward Ubiquitous and Flexible Coverage of UAV-IRS-Assisted NOMA Networks

Chun-Hung Liu and Md Asif Syed
Department of Electrical & Computer Engineering
Mississippi State University, MS, USA
e-mail: chliu@ece.msstate.edu

Lu Wei
Department of Computer Science
Texas Tech University, Lubbock TX, USA
e-mail: luwei@ttu.edu

Abstract—This paper studies methods to achieve a high and flexible coverage performance of a large-scale cellular network. The network shall enable unmanned aerial vehicles (UAVs) for non-orthogonal multiple access (NOMA) transmission enhancement so as to simultaneously serve two users. The considered scenario consists of a network with a tier of base stations and UAVs. Each UAV is mounted with an intelligent reflecting surface (IRS) in order to serve as an aerial IRS reflecting signals between a base station and a user in the network. All the UAVs in the network are deployed based on a newly proposed three-dimensional (3D) point process leading to a tractable yet accurate analysis of the association statistics, which is otherwise difficult to analyze due to the mobility of UAVs. In light of this, we also analyze the downlink coverage of UAV-IRS-assisted NOMA transmission for two users and derive the corresponding coverage probabilities. Our coverage analyses shed light on the optimal allocations of transmit power between NOMA users and UAVs to accomplish the goal of ubiquitous and flexible NOMA transmission. We also conduct numerical simulations to validate our coverage analysis results while demonstrating the improved coverage performance achieved by aerial IRSs.

Index Terms—Coverage, Unmanned Aerial Vehicle, Intelligent Reflecting Surface, NOMA.

I. INTRODUCTION

In the past decade, the performance and efficiency of wireless transmission have been significantly improved thanks to the technological advances enhancing the quality of received signals of communication systems. The multi-antenna technology, for example, is able to considerably boost the signal strength of a point-to-point wireless link by exploiting the spatial and temporal diversity. The cognitive radio technology can improve the efficiency of spectrum utilization. Moreover, the millimeter wave technology leads to a gigabit-level transmission rate in 5G systems. These technologies were developed by following the core idea of strengthening the desired signals on both the transmitter and receiver sides. As these technologies are becoming mature, there may not be much room for further significant improvement for wireless transmission. We are thus imperative to seek other non-traditional feasible solutions to benefiting wireless transmission when embarking on the journey of investigating next-generation wireless networks.

The work of C.-H. Liu and M. A. Syed was supported in part by the U.S. National Science Foundation (NSF) under Award CNS-2006453 and in part by Mississippi State University under Grant ORED 253551-060702. The work of L. Wei was supported in part by the NSF under Award CNS-2006612.

There is a often neglected approach that is able to directly improve wireless signal transmission. The idea is to annihilate the impact of various environmental factors, such as, blockage, topography, and weather on the transmission performance of wireless channels. Recently, such an approach has been more viable in light of the advance in manufacturing intelligent reflecting surface (IRSs). An IRS is a passive device that can be manipulated to alter and reflect its incident signals with a negligible power loss. Therefore, the deployment of IRSs in wireless networks enables a more controllable wireless transmission environment, thereby nullifying the uncontrollable nature of wireless channels [1]–[3]. Accordingly, how to efficiently and economically deploy IRSs to achieve a satisfactory coverage of all users in the wireless network becomes a challenging task. This is especially true when some special transmission techniques, such as NOMA, are employed in the wireless network. To investigate the impact of IRSs deployment on the coverage of a wireless NOMA network, in this paper we propose a three-dimensional (3D) large-scale wireless network enabling UAVs mounted with an IRS to reflect NOMA signals from base stations to users on the ground. To the best of our knowledge, the coverage problem of large-scale wireless networks using UAV-IRS-assisted NOMA has not been addressed in the literature.

There are a few recent works focusing on the special case of a single-cell wireless network using UAVs with IRSs as intelligent and energy-efficient mobile devices [4]–[7]. There, a UAV is utilized to improve the channel quality by adjusting its hovering position between a base station and a user. In particular, reference [4] studied downlink UAV-IRS-assisted communication, where the coverage probability and ergodic capacity were studied using an elevation-angle-dependent path-loss model and the bounds of the average signal-to-noise power ratio were also derived. In [5], an integrated downlink model of a UAV-IRS-assisted cellular network when considering three different modes (i.e., UAV-only, IRS-only, and integrated UAV-IRS modes) was proposed, where the corresponding outage probability, ergodic capacity, and energy efficiency were analyzed. Reference [6] investigated the symbol error rate and outage probability of multi-layer IRS-assisted UAV communication without perfect channel state information, where it was shown that the communication performance between UAVs can be improved when using a

large number of IRS elements for phase error mitigation. Although the aforementioned works pave the way to the understanding of UAV-assisted communication, these results may not be applicable to the large-scale multi-cell wireless network.

The main contributions of this paper are summarized as follows. We first propose a large-scale 3D model of UAV-IRS-assisted NOMA networks consisting of base stations (BSs) on the ground and UAVs in the sky. We then analyze the resulting statistics of the 3D UAV association scheme considering channel blocking indicating how densely UAVs and users should be deployed and distributed for a highly feasible UAV-IRS-assisted NOMA transmission. The maximum achievable coverage probability of a near user and a far user in the cell of a BS is derived in the scenario when the BS schedules a UAV to reflect signals to the far user. The derived coverage probability helps the design of optimal power allocation policies and the formulation of an optimization problem of UAV positioning for a highly ubiquitous and flexible coverage of users in the network. More importantly, our analytical findings reveal the fact that UAV-IRS-assisted communication brings more flexibility for BSs when paring with NOMA users.

II. SYSTEM MODEL

We consider a cellular network with a tier of BSs deployed on the ground, a tier of UAVs deployed in the sky, and users scattered on the ground. All the users are distributed by following a 2D homogeneous Poisson point process (HPPP) of density μ and all the BSs form an independent HPPP Φ_B of density λ_B , which can be written as the following set

$$\Phi_B \triangleq \{B_i \in \mathbb{R}^2 : i \in \mathbb{N}_+\}, \quad (1)$$

where B_i denotes BS i and its ground location. Each user associates with its nearest BS. Without loss of generality, consider a typical BS B_o located at the origin, where the following formulation and analyses will be expressed via the location of B_o . All the UAVs are deployed based on the following 3D point processes proposed in our previous work [8]:

$$\Phi_D \triangleq \left\{ D_j \in \mathbb{R}^2 \times \left(0, \frac{\pi}{2}\right) : D_j = (X_j, \Theta_j), X_j \in \mathbb{R}^2, \Theta_j \in \left(0, \frac{\pi}{2}\right), j \in \mathbb{N}_+ \right\}, \quad (2)$$

where D_j denotes UAV j and its 3D location, X_j is the projection of D_j on the ground, and Θ_j is the elevation angle from B_o to D_j . All the projections of the UAVs (i.e., set $\{X_j \in \mathbb{R}^2 : j \in \mathbb{N}_+\}$) are assumed to form an independent 2D HPPP of density λ_D .

A. UAV Channel Model and UAV Association

A channel (link) between two spatial points is called a line-of-sight (LoS) channel if it is not visually blocked from one point to the other. Here, a low-altitude-platform (LAP) communication scenario is considered so that the LoS model

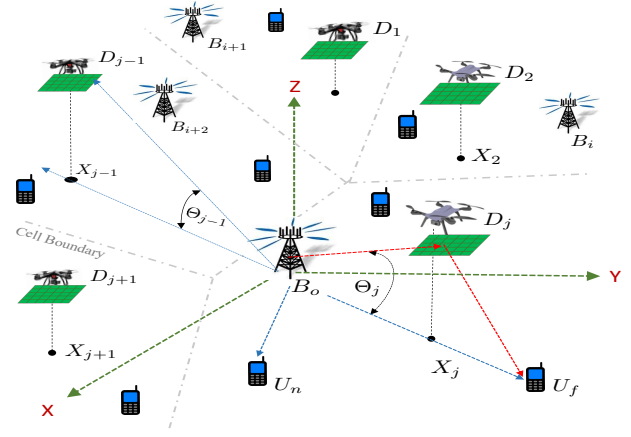


Fig. 1. The proposed network model consists of a tier of BSs, a tier of UAVs mounted with an IRS, and users. A typical BS B_o is located at the origin and it adopts NOMA transmission to serve a near user U_n and a far user U_f . A UAV D_j associating with B_o is scheduled to reflect signals between B_o and U_f . To minimize the path loss of the reflected signals between B_o and U_f , D_j hovers right above the middle point of the distance between B_o and U_f with an elevation angle Θ_j , i.e., $\|X_j\| = \|D_j\| \cos(\Theta_j) = \frac{1}{2}\|U_f\|$.

of a 3D channel in [9] is adopted¹, which gives rise to the LoS probability of a 3D link between UAV j and any ground point $Y_k \in \mathbb{R}^2$ given by

$$\rho(\Theta_{kj}) = \frac{1}{1 + c_2 \exp(-c_1 \Theta_{kj})}, \quad (3)$$

where $\Theta_{kj} \in (0, \frac{\pi}{2})$ is the elevation angle between Y_k and D_j , c_1 and c_2 are environment-dependent positive constants (for urban, rural, etc.). Each UAV associates with a BS in Φ_B that provides it with the strongest average power. As such, D_j associates with BS B_o whenever B_o is satisfied with the following association scheme:

$$B_o = \arg \max_{i: B_i \in \Phi_B} \mathbb{E} \left[\frac{P H_{ij} L_{ij}}{\|B_i - D_j\|^\alpha} \middle| B_i \right], \quad (4)$$

where P is the transmit power of a BS, $\|B_i - D_j\|$ denotes the Euclidean distance between B_i and D_j , $L_{ij} \in \{1, \eta\}$ is a Bernoulli random variable that is equal to 1 if the link between B_i and D_j is a non-LoS (NLoS) one and η otherwise, $\alpha > 2$ is the path-loss exponent of a link, and H_{ij} denotes the fading channel gain from B_i to D_j . Throughout this paper, all the fading channel gains are assumed to be i.i.d. exponential random variables (RVs) with unit mean, e.g., $H_{ij} \sim \exp(1)$ for all $i, j \in \mathbb{N}_+$. Note that $\eta > 1$ is used to model the enhanced channel gain of a 3D LoS link in contract to that of a 3D NLoS link so that it is referred to as the 3D LoS channel enhancement factor². Also note that L_{ij} and H_{ij} are independent since L_{ij} is used to characterize whether the link

¹In this paper, we assume that the 3D ground-to-air channels and the 3D air-to-ground channels are reciprocal and thereby they adopt the same LAP model.

²To simplify the complexity of modeling and analysis, this paper assumes that all the 2D (ground-to-ground) channels are NLoS and adopt the same path-loss model as that used in the 3D NLoS channel model proposed in (4).

between D_j and B_i is LoS and it is completely determined for a given B_i and D_j . Hence, the definition (4) is reduced to

$$\begin{aligned} B_o &= \arg \max_{i: B_i \in \Phi_B} \frac{PL_{ij} \mathbb{E}[H_{ij}]}{\|B_i - D_j\|^\alpha} \\ &= \arg \min_{i: B_i \in \Phi_B} L_{ij}^{-\frac{1}{\alpha}} \|B_i - D_j\|, \end{aligned} \quad (5)$$

where the second equality is obtained because constants P and $\mathbb{E}[H_{ij}] = 1$ do not affect the association result. Note that the distribution of L_{ij} depends on the elevation angle between B_i and D_j according to (3) and all L_{ij} 's are assumed to be i.i.d.

Using the expression of B_o in (5), the numbers of users and UAVs become RVs, whose distributions are shown in the following theorem.

Theorem 1. *Let M and N denote the number of the users and the number of the UAVs associating with BS B_o , respectively. The probability mass function (PMF) of M can be accurately approximated by*

$$\mathbb{P}[M = m] \approx \frac{\Gamma(m + \frac{7}{2})}{m! \Gamma(\frac{7}{2})} \left(\frac{2\mu}{7\lambda_B} \right)^m \left(1 + \frac{2\mu}{7\lambda_B} \right)^{-(m + \frac{7}{2})}, \quad (6)$$

where $\Gamma(z) \triangleq \int_0^\infty x^{z-1} e^{-x} dx$ is the Gamma function. If the elevation angle Θ_{ij} between B_i and D_j is independent of the distance between B_i and the projection X_j of D_j (i.e. $\|B_i - X_j\|$) and all Θ_{ij} 's are i.i.d. for all $i, j \in \mathbb{N}_+$, the PMF of N can be accurately approximated by

$$\mathbb{P}[N = n] \approx \frac{\Gamma(n + \frac{7}{2})}{n! \Gamma(\frac{7}{2})} \left(\frac{2\lambda_D}{7w_b\lambda_B} \right)^n \left(1 + \frac{2\lambda_D}{7w_b\lambda_B} \right)^{-(n + \frac{7}{2})}, \quad (7)$$

where w_b is defined as

$$\begin{aligned} w_b &\triangleq \mathbb{E} \left\{ \cos^2(\Theta) \left[\rho(\Theta) \left(1 - \eta^{\frac{2}{\alpha}} \right) + \eta^{\frac{2}{\alpha}} \right] \right\} \\ &\quad \times \mathbb{E} \left\{ \sec^2(\Theta) \left[\rho(\Theta) \left(1 - \eta^{-\frac{2}{\alpha}} \right) + \eta^{-\frac{2}{\alpha}} \right] \right\}, \end{aligned} \quad (8)$$

with the distribution of RV Θ being the same as that of Θ_{ij} .

Proof: See Appendix A. ■

From Theorem 1, we see that $\mathbb{P}[M = 0] \approx \mathbb{P}[N = 0] \approx 0$ when μ and λ_D are very large. Namely, each BS is almost surely associated with at least one UAV and one user if the densities of the users and the UAVs are sufficiently large. Thus, in this scenario we do not need to consider a cellular network having the phenomenon of *void* cells in the network [10]³. Moreover, each UAV is mounted with an IRS consisting of R reflecting elements so that it essentially serves as an aerial IRS that helps reflect signals between a BS and users. For example, D_j associating with B_o uses an IRS to reflect the signals between B_o and a user associating with B_o . An illustration of the network model is depicted in Fig. 1.

³The cell of a BS is called a void cell if no users and UAVs associate with the BS.

B. Downlink UAV-IRS-Assisted NOMA Transmission

Here, we investigate the downlink transmission performance from a BS to its users when a UAV associating with the BS is used to assist the downlink transmission via an IRS. Suppose the densities of the users and the UAVs are sufficiently large so that there are almost surely at least one UAV and two users associating with B_o in the cell of B_o according to the statistics of 2D and 3D user association result in Theorem 1. We are interested in the scenario when B_o is associated with multiple users and would like use the *power-domain* NOMA to simultaneously transmit different data streams to different users through the same frequency band. In each of the downlink transmission slots, B_o schedules two users, i.e., a near user and a far user, in its cell for NOMA transmission, which also schedules UAV D_j to reflect the signals from B_o to the far user. Suppose the network is *interference-limited* and each UAV is able to control its IRS to merely reflect the signals to its desired user so that the signals reflected do not interfere with any other user in the network.

Let U_n and U_f denote respectively the near user and the far user scheduled by B_o in a transmission slot. Assuming each BS adopts different radio resource blocks to transmit different NOMA signals in its cell and each user is able to remove some NOMA interference via successive interference cancellation (SIC) of the received signals. Then, the *achievable* signal-to-interference ratio (SIR) of the near user U_n can be defined as⁴

$$\gamma_n \triangleq \frac{P_n G_{on} \|B_o - U_n\|^{-\alpha}}{\mathbb{1}(P_f < P_n) I_{N,n} + I_{B,n}}, \quad (9)$$

where P_n is the power for the transmission of the desired signal of U_n , $G_{on} \sim \exp(1)$ denotes the fading channel gain of the link from B_o to U_n , $I_{N,n} \triangleq P_f G_{on} \|B_o - U_n\|^{-\alpha}$ is the intra-cell NOMA interference received by U_n , P_f is the power used to transmit the desired signal of U_f , $\mathbb{1}(\mathcal{A})$ is the indicator function that equals one if event \mathcal{A} is true and zero otherwise, $I_{B,n} \triangleq \sum_{i: B_i \in \Phi_B \setminus B_o} P G_{in} \|B_i - U_n\|^{-\alpha}$ denotes the inter-cell interference from the BSs in the network, and $G_{in} \sim \exp(1)$ is the fading channel gain from B_i to U_n . We also notice that $P_f + P_n = P$.

Since UAV D_j is scheduled by B_o to reflect the signals from B_o to U_f and the fact that the path-loss model of a metasurface-based IRS is considered [1], the unit signal power reflected by D_j and received by U_f is expressed as

$$W_f \triangleq H_f L_{oj} L_{jf} (\|B_o - D_j\| + \|D_j - U_f\|)^{-\alpha}. \quad (10)$$

Here, H_f is the *equivalent* fading channel gain that characterizes channel fading of the reflected channel from B_o to U_f through D_j . Also, H_f is assumed to be a Gamma RV with shape R and rate 1 (i.e., $H_f \sim \text{Gamma}(R, 1)$) in that D_j is able to control its IRS with R reflecting elements such that all

⁴When $P_f > P_n$, U_n is able to perform SIC so as to remove $I_{N,n}$ such that γ_n increases. Otherwise, $I_{N,n}$ remains in (9) and γ_n cannot thus be improved by SIC.

the R signals reflected by its IRS can be coherently combined at U_f . As such, the achievable SIR of U_f can be defined as

$$\gamma_f \triangleq \frac{P_f[W_f + G_{of}\|B_o - U_f\|^{-\alpha}]}{\mathbb{1}(P_n < P_f)I_{N,f} + I_{B,f}}, \quad (11)$$

where $G_{of} \sim \exp(1)$ is the fading channel gain from B_o to U_f , $I_{N,f} \triangleq P_n[W_f + G_{of}\|B_o - U_f\|^{-\alpha}]$ denotes the intra-cell NOMA interference received by U_f , $I_{B,f} \triangleq \sum_{i: B_i \in \Phi_B \setminus B_o} P G_{if} \|B_i - U_f\|^{-\alpha}$ is the inter-cell interference. Note that UAV D_j is able to fly to the position whose projection is in the middle point of the straight path between B_o and U_f . In this way, the distance between B_o and U_f through D_j is minimal for a given elevation angle, as shown in Fig. 1. As a result, the coverage probability of the far user can be further increased by the mobility of UAVs. In the following section, we will use γ_n and γ_f to first define the coverage probabilities of the near and far users before providing insights into power allocations between the two users and UAVs for an improved NOMA transmission.

III. ACHIEVABLE COVERAGE OF UAV-IRS-ASSISTED DOWNLINK NOMA

According to the definition (9), for a minimum required SIR threshold of a successful decoding $\beta > 0$, the coverage probabilities of the near user and the far user are defined as

$$c_n \triangleq \mathbb{P}[\gamma_n \geq \beta] \quad \text{and} \quad c_f \triangleq \mathbb{P}[\gamma_f \geq \beta], \quad (12)$$

respectively. The explicit expressions of c_n and c_f are given in the following theorem.

Theorem 2. *The coverage probability c_n of the near user is*

$$c_n = \begin{cases} \left[1 + \Psi\left(\frac{2}{\alpha}, \frac{P\beta}{(P_n - \beta P_f)}\right) \right]^{-1}, & P_n > \max\{1, \beta\}P_f \\ \left[1 + \Psi\left(\frac{2}{\alpha}, \frac{P\beta}{P_n}\right) \right]^{-1}, & P_n \leq P_f \end{cases}, \quad (13)$$

where the function $\Psi(x, y)$ for $x, y > 0$ is defined as

$$\Psi(x, y) \triangleq y^x \left(\frac{\pi x}{\sin(\pi x)} - \int_0^{y^{-x}} \frac{dz}{1 + z^{\frac{1}{x}}} \right). \quad (14)$$

If the number of the reflecting elements of an IRS is sufficiently large (i.e., $R \gg 1$), the coverage probability of the far user defined in (12) can be accurately approximated by (15) as shown on top of next page, where τ_i is defined as

$$\tau_i = \begin{cases} \frac{\eta^i (P_f - \beta P_n)}{\beta P} \cos^\alpha(\Theta), & P_f > \max\{1, \beta\}P_n \\ \frac{\eta^i P_f}{\beta P} \cos^\alpha(\Theta), & P_f \leq P_n \end{cases}, \quad (16)$$

with Θ having the same distribution as Θ_j .

Proof: See Appendix B. ■

A few interesting and crucial observations of Theorem 2 are in order. First, c_f can be greater than c_n as long as the signals reflected from the UAV to the far user have been sufficiently enhanced by making R large and positioning the UAV channels as a LoS one. Hence, both of the users have

TABLE I
NETWORK PARAMETERS FOR SIMULATION [9]

Transmit Power of BSs (W) P	30
Density of Φ_B (BSs/m ²) λ_B	1×10^{-5}
Density of Φ_D (UAV/m ²) λ_D	1×10^{-4}
Number of Reflecting Elements R	8, 16, 32 (see figures)
Path-loss Exponent α	3
Parameters (c_1, c_2) in (3) for Suburban	(24.5811, 39.5971)
3D LoS Channel Enhancement Factor η	2.5
SIR Threshold β	0.5

a chance to perform SIC for SIR improvement depending on the transmit power allocation⁵. Second, we can conclude that the optimal power allocation policy to maximize c_n in (13) is $P_n > (1 + 2\beta)P_f$, yet the optimal power allocation policy to maximize c_f in (15) is $P_f > (1 + 2\beta)P_n$. These two power control policies are opposite. Nonetheless, it is better to choose the policy that benefits c_n (i.e., $P_n > (1 + 2\beta)P_f$) since c_f can also be significantly improved by the UAV in addition to the optimal power allocation. Third, the result (15) clearly shows how an aerial IRS improves c_f and how the position of a UAV affects c_f . When there is no UAV reflecting the signals from B_o to U_f , c_f will decrease significantly because R , η , and Θ in (15) are reduced to zero, one, and zero, respectively. Besides, c_f will also decrease if a UAV is positioned at a large elevation angle such that $\rho(\Theta)$ is small. Finally, we should maintain $\eta^i \cos^\alpha(\Theta) > 1$ in (16) almost surely in order for the aerial RIS to enjoy the improved NOMA transmission. Namely, the elevation angle of a UAV should be bounded as $0 < \Theta < \cos^{-1}(\eta^{-\frac{2}{\alpha}})$. Consequently, we are able to formulate the following optimization problem for a fixed Θ in (15)

$$\max_{\Theta} c_f(\Theta) \quad \text{s.t.} \quad 0 < \Theta < \cos^{-1}(\eta^{-\frac{2}{\alpha}}) \quad (17)$$

to maximize c_f . This optimization problem is not convex due to the complicated form of c_f in (15), thereby we resort numerical approaches for the solutions. In the following section, we will provide some numerical results to validate the above findings.

IV. NUMERICAL RESULTS AND DISCUSSIONS

In this section, numerical simulation are provided to validate the coverage analyses of the previous section. To simplify the simulation scenarios, the elevation angle from a BS to a UAV is considered to be deterministic when the BS schedules the UAV to reflect its signals to a far user. The main network parameters used for simulation are listed in Table I. We first present the numerical outcomes of the coverage probabilities c_n and c_f in Fig 2 for two different numbers of R , where the elevation angle of the UAV is controlled at $\Theta = 15^\circ$. As can be seen in the figure, all the analytic results match well with their corresponding simulated results, demonstrating the accuracy of the expressions (13) and (15). The coverage probability c_f significantly increases as R increases from 8 to 16, as shown

⁵This is different from the regular NOMA transmission without assisting by an IRS because it needs to allocate more power to the signals of the far user and requests the near user to do SIC so that the SIRs of the near user and the far users are fairly close.

$$c_f \approx \sum_{i=0}^2 \mathbb{E}_{\Theta} \left\{ \rho^i(\Theta) [1 - \rho(\Theta)]^{2-i} \frac{d^{R-1}}{dt^{R-1}} \left(\frac{t^{R-1}}{(R-1)!} \prod_{k=1}^2 \left[1 + \frac{1}{k} \Psi \left(\frac{2}{\alpha}, \frac{1}{t} \right) \right]^{-1} \right) \Big|_{t=\tau_i} \right\}, \quad (15)$$

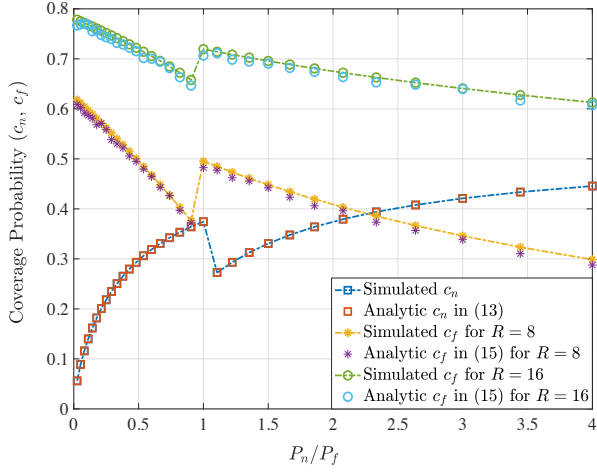


Fig. 2. Simulation results of the coverage probabilities c_n and c_f for different numbers of the reflecting elements of an IRS. The elevation angle of the UAV is controlled at $\Theta = 15^\circ$.

in the figure. In addition, in this simulation c_f is much higher than c_n due to the reflected transmission from the UAV. This observation reveals an important fact: using UAVs with an RIS can remarkably boost the signal strength of users anywhere in the network so that the BS enjoys more flexibility of selecting users to maximize the transmission performance. Moreover, the optimal power allocation policy observed in the previous section, i.e., adopting $P_n > (1 + 2\beta)P_f$ when $c_f > c_n$, can be observed in the figure. Since $\beta = 0.5$, the optimal power allocation policy is $P_n/P_f > 2$ and we can clearly see that the values of c_n when $P_n/P_f > 2$ are larger than those of c_n when $P_n/P_f \leq 2$. Note that although using this policy may not always benefit c_f , we can always increase c_f by adding more reflecting elements of an IRS on a UAV as well as controlling the UAV to improve the channels, as illustrated in Fig. 3.

Fig. 3 shows how the coverage probability c_f varies with the elevation angle of the UAV and the number of the reflecting elements of an IRS. As seen in the figure, c_f improves as R increases and there exists an optimal elevation angle that maximizes c_f for each of the three curves. For example, the three optimal elevation angles for $R = 8, 16, 32$ is about $9.2^\circ, 12.2^\circ$, and 19.5° , which are all smaller than the upper bound $\cos^{-1}(\eta^{-2/\alpha}) = 57.12^\circ$ given in (17). Hence, the optimization problem in (17) admits a feasible solution even though it is not convex, as pointed out in the previous section.

V. CONCLUSION

This paper focuses on studying methods to effectively and significantly improve the coverage of users served by a BS with IRS-assisted NOMA transmission. The statistics of the

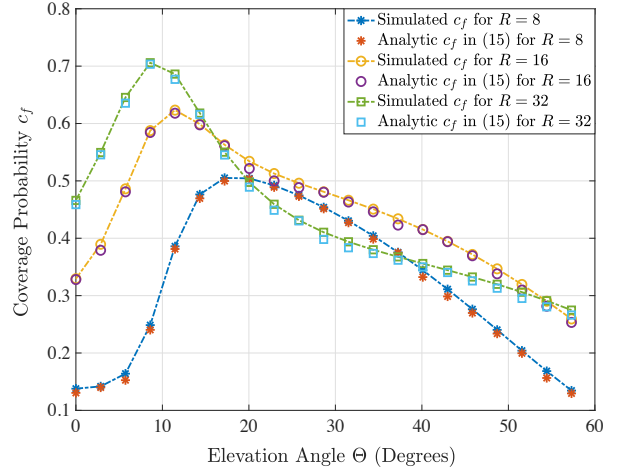


Fig. 3. Simulation results of the coverage probabilities c_n and c_f when the UAV hovers at various elevation angle and the optimal power allocation policy $P_n \geq 2P_f$ is adopted.

3D user association scheme for UAVs that considers LoS and NLoS channels has been analyzed. The results indicate how densely UAVs should be deployed and how the users shall be distributed to ensure an almost surely feasible UAV-IRS-assisted NOMA transmission for a given density of BSs. Each BS is able to adopt NOMA to simultaneously serve a near user and a far user and to schedule a UAV to reflect signals to the far user. The maximum achievable coverage probabilities of the two users are also derived and analyzed. These results provide insights into optimal transmit power allocation between the two users as well as the optimal positioning of UAVs for NOMA transmission anywhere in the network. Our study also sheds light on the fact that UAV-IRS assisted communication brings BSs with more flexibility when paring with NOMA users in the cell.

APPENDIX

A. Proof of Theorem 1

Since each user associates with its nearest BS, the result in (6) can be readily obtained from Lemma 1 in [11]. To show the outcome in (7), we first need to rewrite (5) as

$$\begin{aligned} B_o &= \arg \min_{i: B_i \in \Phi_B} L_{ij}^{-\frac{2}{\alpha}} \|B_i - D_j\|^2 \\ &\stackrel{(a)}{=} \arg \max_{i: B_i \in \Phi_B} L_{ij} \sec^{-\alpha}(\Theta_{ij}) \|B_i - X_j\|^{-\alpha} \\ &\stackrel{(b)}{=} \arg \max_{i: B_i \in \Phi_B} L_{ij} \cos^\alpha(\Theta_{ij}) \|B_i\|^{-\alpha}, \end{aligned}$$

where (a) is obtained due to $\|B_i - D_j\| = \sec(\Theta_{ij}) \|B_i - X_j\|$ and (b) follows by considering X_j as the origin and the fact that the statistic property evaluated at any point in an HPPP

is the same according to the Slivnyak theorem [12]. If Θ_{ij} is independent of $\|B_i - X_j\|$, we can apply the result of Lemma 1 in [11] to find w_b in (8) as follows

$$\begin{aligned} w_b &= \mathbb{E} \left[(L_{ij} \cos^\alpha(\Theta_{ij}))^{\frac{2}{\alpha}} \right] \mathbb{E} \left[(L_{ij} \cos^\alpha(\Theta_{ij}))^{-\frac{2}{\alpha}} \right] \\ &= \mathbb{E} \left[L^{\frac{2}{\alpha}} \cos^2(\Theta) \right] \mathbb{E} \left[L^{-\frac{2}{\alpha}} \sec^2(\Theta) \right], \end{aligned}$$

which equals to (8) by employing $\rho(\cdot)$ in (3) of the above expression since all $L_{ij} \cos^\alpha(\Theta_{ij})$'s are independent.

B. Proof of Theorem 2

According to (9) and (12), if $P_n > P_f$, the near user can not perform SIC to remove $I_{N,n}$ and c_n are thus written as follows:

$$\begin{aligned} c_n &= \mathbb{P}[\gamma_n \geq \beta | P_n > P_f] = \mathbb{P} \left[\frac{P_n G_n \|U_n\|^{-\alpha}}{I_{N,n} + I_{B,n}} \geq \beta \right] \\ &= \mathbb{P} \left[I_{B,n} \leq \left(\frac{1}{\beta} - \frac{P_f}{P_n} \right)^+ P_n G_n \|U_n\|^{-\alpha} \right] \\ &= \mathbb{P} \left[\sum_{i: B_i \in \Phi_B \setminus B_o} \frac{P G_{in} \|U_n\|^\alpha}{P_n \|B_i - U_n\|^\alpha} \leq \left(\frac{1}{\beta} - \frac{P_f}{P_n} \right)^+ G_n \right] \\ &\stackrel{(a)}{=} \mathbb{E} \left[\exp \left\{ - \frac{P\beta}{(P_n - \beta P_f)^+} \sum_{i: B_i \in \Phi_B \setminus B_o} \frac{G_{in} \|U_n\|^\alpha}{\|B_i - U_n\|^\alpha} \right\} \right] \\ &\stackrel{(b)}{=} \left[1 + \Psi \left(\frac{2}{\alpha}, \frac{P\beta}{(P_n - \beta P_f)^+} \right) \right]^{-1}, \quad (\text{A.1}) \end{aligned}$$

where $x^+ \triangleq \max\{0, x\}$, (a) follows from the fact $G_n \sim \exp(1)$ and (b) is obtained by using the result $\|U_n\|^2 \sim \exp(\pi\lambda_B)$ before applying the derivation techniques devised in [11] based on the Probability Generating Functional (PGFL) of an HPPP. Hence, c_n in (13) for the case of $P_n > P_f$ is found. When $P_f \geq P_n$, the near user can perform SIC to remove $I_{N,n}$ from γ_n so that the coverage probability of the near user in (13) for the case of $P_f \geq P_n$ can be readily obtained by substituting $P_f = 0$ into the coverage probability (A.1).

To derive c_f , we first rewrite W_f in (10) as $W_f = H_f L_{oj} L_{jf} (\sec(\Theta) \|U_f\|)^{-\alpha}$ by considering UAV D_j hovering above the middle point of the straight path between B_o and U_f with an elevation angle Θ_j . Then, assuming R is large enough such that $W_f = H_f L_{oj} L_{jf} (\sec(\Theta_j) \|U_f\|)^{-\alpha}$ is almost surely much larger than $G_f \|U_f\|^{-\alpha}$ (i.e., $W_f \gg G_f \|U_f\|^{-\alpha}$). Accordingly, we can accurately express c_f in (12) by neglecting $G_f \|U_f\|^{-\alpha}$ and conditioning on $L_{oj} L_{jf}$ for the case of $P_n < P_f$, $B_0 = \mathbf{0}$ as follows:

$$\begin{aligned} c_f &\approx \mathbb{P} \left[\frac{P_f W_f}{P_n W_f + I_{B,f}} \geq \beta \right] = \mathbb{P} \left[W_f \leq \frac{\beta I_{B,f}}{(P_f - \beta P_n)^+} \right] \\ &= \mathbb{P} \left[H_f \geq \frac{\beta I_{B,f} \sec^\alpha(\Theta_j) \|U_f\|^\alpha}{(P_f - \beta P_n)^+ L_{oj} L_{jf}} \right] \\ &\stackrel{(c)}{=} \frac{d^{R-1}}{dt^{R-1}} \left\{ \frac{t^{R-1}}{(R-1)!} \mathbb{E} \left[e^{-\pi\lambda_B \Psi(\frac{2}{\alpha}, \frac{1}{t}) \|U_f\|^2} \right] \right\} \Big|_{t=t_o}, \quad (\text{A.2}) \end{aligned}$$

where (c) is obtained by applying the derivation techniques in the proof of Proposition 1 in [13] and $t_o = \frac{(P_f - \beta P_n)^+ L_{oj} L_{jf}}{\beta P \sec^\alpha(\Theta_j)}$. Furthermore, since $\|U_f\| \geq \|U_n\|$ and we know $\mathbb{E}[\exp(-\pi\lambda_B s \|U_f\|^2)] = \frac{2}{(s+2)(s+1)}$ for $s > 0$ according to the proof of Proposition 1 in [13], we can infer the following result:

$$\mathbb{E} \left[e^{-\pi\lambda_B \Psi(\frac{2}{\alpha}, \frac{1}{t}) \|U_f\|^2} \right] = \prod_{k=1}^2 \left[1 + \frac{1}{k} \Psi \left(\frac{2}{\alpha}, \frac{1}{t} \right) \right]^{-1}.$$

Substituting the above result into (A.2) yields

$$c_f \approx \frac{d^{R-1}}{dt^{R-1}} \left\{ \frac{t^{R-1}}{(R-1)!} \prod_{k=1}^2 \left[1 + \frac{1}{k} \Psi \left(\frac{2}{\alpha}, \frac{1}{t} \right) \right]^{-1} \right\} \Big|_{t=t_o}.$$

Finally, considering the RV $L_{oj} L_{jf} \in \{1, \eta, \eta^2\}$, where the independence between L_{oj} and L_{jf} leads to the expression of c_f in (15) for the case of $P_n > P_f$. For the case $P_f \leq P_n$, the substitution $P_n = 0$ in (15) for the case of $P_n > P_f$ gives rise to the expression of c_f in (15).

REFERENCES

- [1] M. ElMossallamy, H. Zhang, L. Song, K. G. Seddik, Z. Han, and G. Y. Li, "Reconfigurable intelligent surfaces for wireless communications: Principles, challenges, and opportunities," *IEEE Trans. Cognitive Commun. and Netw.*, vol. 6, no. 3, pp. 990–1002, Sep. 2020.
- [2] Y. Liu, X. Liu, X. Mu, T. Hou, J. Xu, M. D. Renzo, and N. Al-Dahir, "Reconfigurable intelligent surfaces: Principles and opportunities," *IEEE Commun. Surveys Tuts.*, vol. 23, no. 3, pp. 1546–1577, Thirdquarter 2021.
- [3] E. Basar and I. Yildirim, "Reconfigurable intelligent surfaces for future wireless networks: A channel modeling perspective," *IEEE Wireless Commun.*, vol. 28, no. 3, pp. 108–114, Jun. 2021.
- [4] A. Mahmoud, S. Muhaidat, P. C. Sofotasios, I. Abualhaol, O. A. Dobre, and H. Yanikomeroglu, "Intelligent reflecting surfaces assisted UAV communications for IoT networks: Performance analysis," *IEEE Trans. Green Commun. Netw.*, vol. 5, no. 3, pp. 1029–1040, 2021.
- [5] T. Shafique, H. Tabassum, and E. Hossain, "Optimization of wireless relaying with flexible UAV-Borne reflecting surfaces," *IEEE Trans. Commun.*, vol. 69, no. 1, pp. 309–325, 2021.
- [6] M. Al-Jarrah, A. Al-Dweik, E. Alsusa, Y. Iraqi, and M.-S. Alouini, "On the performance of IRS-Assisted multi-layer uav communications with imperfect phase compensation," *IEEE Trans. Commun.*, pp. 1–1, 2021.
- [7] K. Guo, C. Wang, Z. Li, D. W. K. Ng, and K.-K. Wong, "Multiple UAV-Borne IRS-Aided millimeter wave multicast communications: A joint optimization framework," *IEEE Communications Letters*, pp. 1–1, 2021.
- [8] C.-H. Liu, D.-C. Liang, M. A. Syed, and R.-H. Gau, "A 3D tractable model for UAV-Enabled cellular networks with multiple antennas," *IEEE Trans. Wireless Commun.*, vol. 20, no. 6, pp. 3538–3554, Jun. 2021.
- [9] A. Al-Hourani, S. Kandeepan, and S. Lardner, "Optimal LAP altitude for maximum coverage," *IEEE Wireless Commun. Lett.*, vol. 3, no. 6, pp. 569–572, Dec. 2014.
- [10] C.-H. Liu and L.-C. Wang, "Optimal cell load and throughput in green small cell networks with generalized cell association," *IEEE J. Sel. Areas Commun.*, vol. 34, no. 5, pp. 1058–1072, May 2016.
- [11] C.-H. Liu and K. L. Fong, "Fundamentals of the downlink green coverage and energy efficiency in heterogeneous networks," *IEEE J. Sel. Areas Commun.*, vol. 34, no. 12, pp. 3271–3287, Dec. 2016.
- [12] S. N. Chiu, D. Stoyan, W. S. Kendall, and J. Mecke, *Stochastic Geometry and Its Applications*, 3rd ed. New York: John Wiley and Sons, Inc., 2013.
- [13] C.-H. Liu and D.-C. Liang, "Heterogeneous networks with power-domain NOMA: Coverage, throughput, and power allocation analysis," *IEEE Trans. Wireless Commun.*, vol. 17, no. 5, pp. 3524–3539, May 2018.